Electronic Supplementary Material (ESI) for Nanoscale.

Supplementary Information

UV-SWIR Broad Range Photodetectors Made from Few-layer α-In_2Se_3 Nanosheets

Bin Tang[a,c], Linfang Hou[b], Mei Sun[a], Fengjiao Lv[a], Jianhui Liao*[a], Wei Ji*[b] and Qing Chen*[a]

[a.] *Key Laboratory for the Physics and Chemistry of Nanodevices and Department of Electronics, Peking University, Beijing 100871, China*

[b.] *Beijing Key Laboratory of Optoelectronic Functional Materials & Micro-Nano Devices and Department of Physics, Renmin University of China, Beijing 100872, China*

[c.] *Academy for Advanced Interdisciplinary Studies, Peking University, Beijing 100871, China*

E-mail: jianhui.liao@pku.edu.cn, wji@ruc.edu.cn, qingchen@pku.edu.cn

Contents

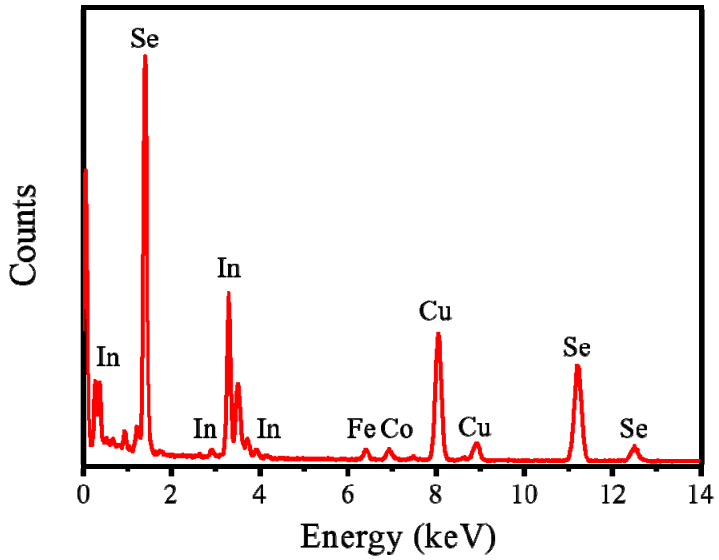

Figure S1. The energy-dispersive X-ray spectrometry (EDS) of a typical In_2Se_3 nanosheet. The nanosheet was prepared by using the mechanical exfoliation with Scotch tape and blue Nitto tapes. The Fe and Co signals come from the sample holder and Cu signal comes from the TEM Cu-grid supporting the holey carbon film.

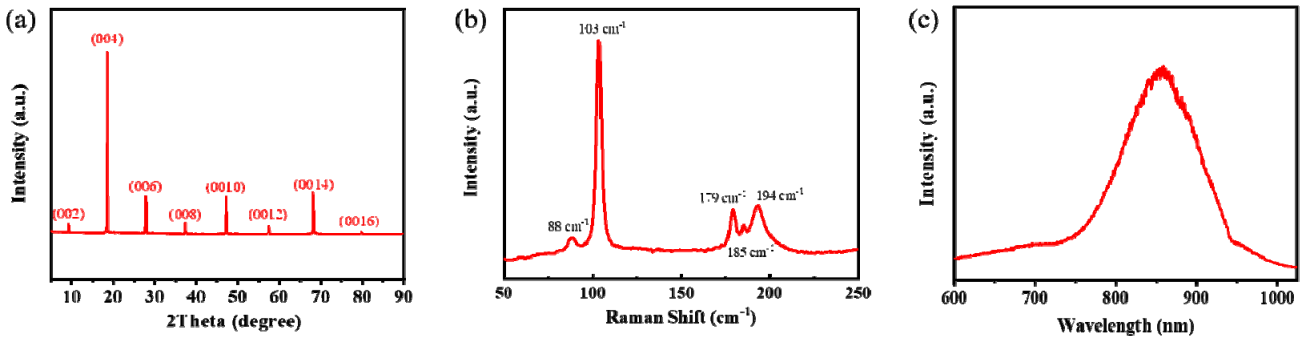

Figure S2. X-ray diffraction, Raman spectrum and PL spectrum of α-In_2Se_3. a) Typical X-ray diffraction spectrum of the bulk single crystal α-In_2Se_3 at T = 300 K and ambient conditions. b) Raman spectrum of exfoliated few-layered α-In_2Se_3 at T = 300 K and ambient conditions. The power of the 633 nm laser is 5.96 mW. c) The PL spectrum the bulk single crystal α-In_2Se_3 measured using 532 nm wavelength laser and 1 mW at room temperature under ambient conditions. The typical integration time for collecting the spectrum is 60 s.

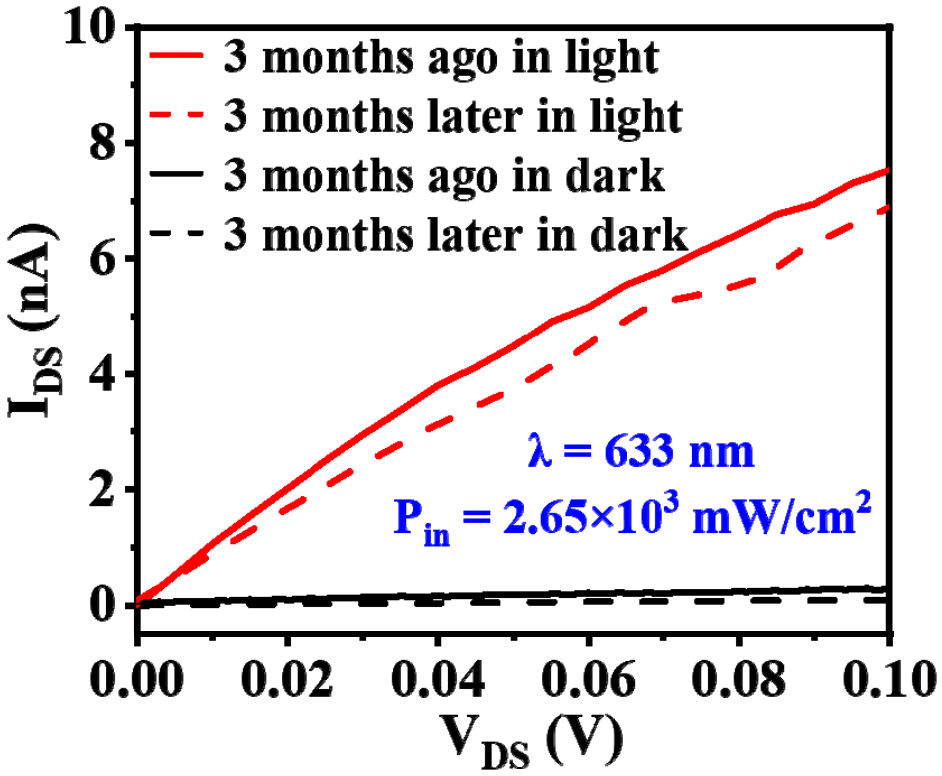

Figure S3. The stability characterization of In_2Se_3 transistors. We compare the photocurrent before and after three months' storage. The solid and dotted lines indicate the dark current and the current under light illumination of the In_2Se_3 photodetector before and after three months' storage, respectively. The measurements were all performed in vacuum. The laser wavelength was 633 nm. The power density of the incident light was 2.65×10^3 mW cm^{-2}.

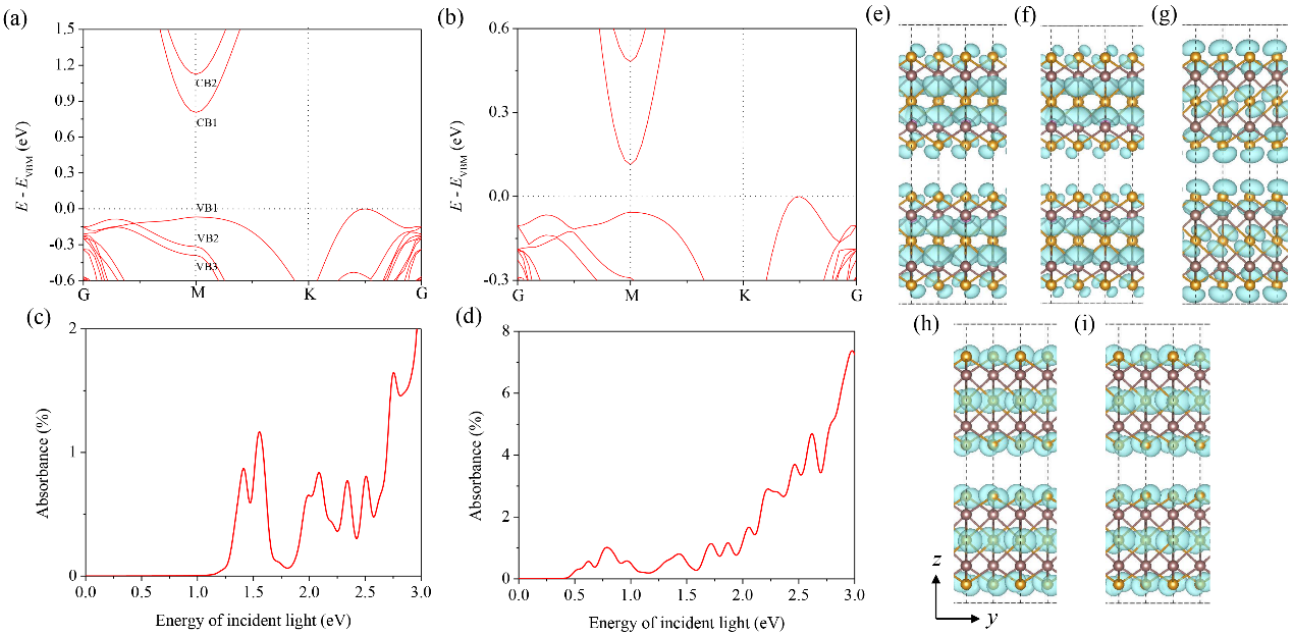

Figure S4. DFT calculation of bulk structure. a) Band structure and (c) optical absorption spectrum calculated by HSE06 functional. b) Band structure and (d) optical absorption spectrum calculated by optB86b-vdW functional. Visualization of orbitals (e-i) CB2, CB1, VB1, VB2, VB3 of bulk structure by charge density iso-surface for First Brillouin zone M point.

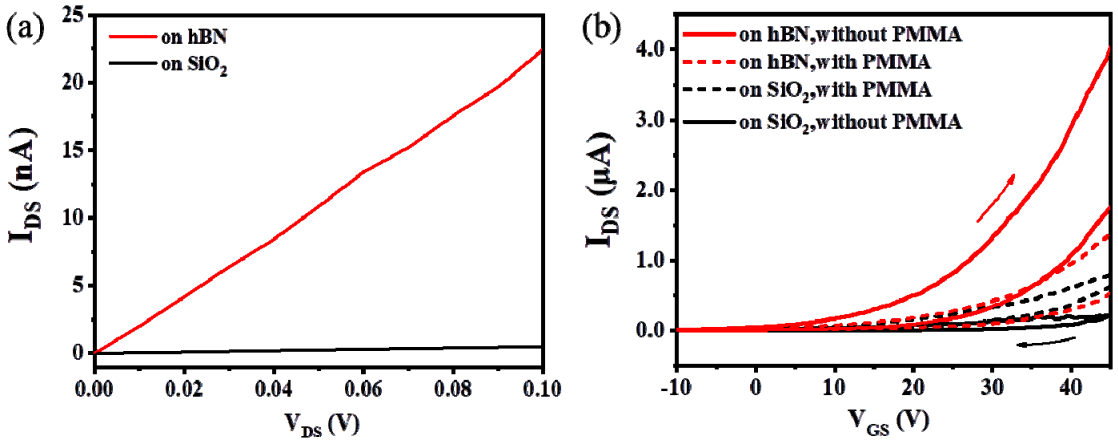

Figure S5. Device characterization of few-layered α-In_2Se_3 transistors under different conditions. a) Output curves of In_2Se_3 nanosheets on different substrates under the bias V_{DS} = 0.1 V, V_{GS} = 0 V. b) Transfer curves of In_2Se_3 nanosheets on different substrates with/without PMMA coating. The voltage between source and drain is V_{DS} = 0.3 V. All measurements were performed at room temperature under ambient conditions.

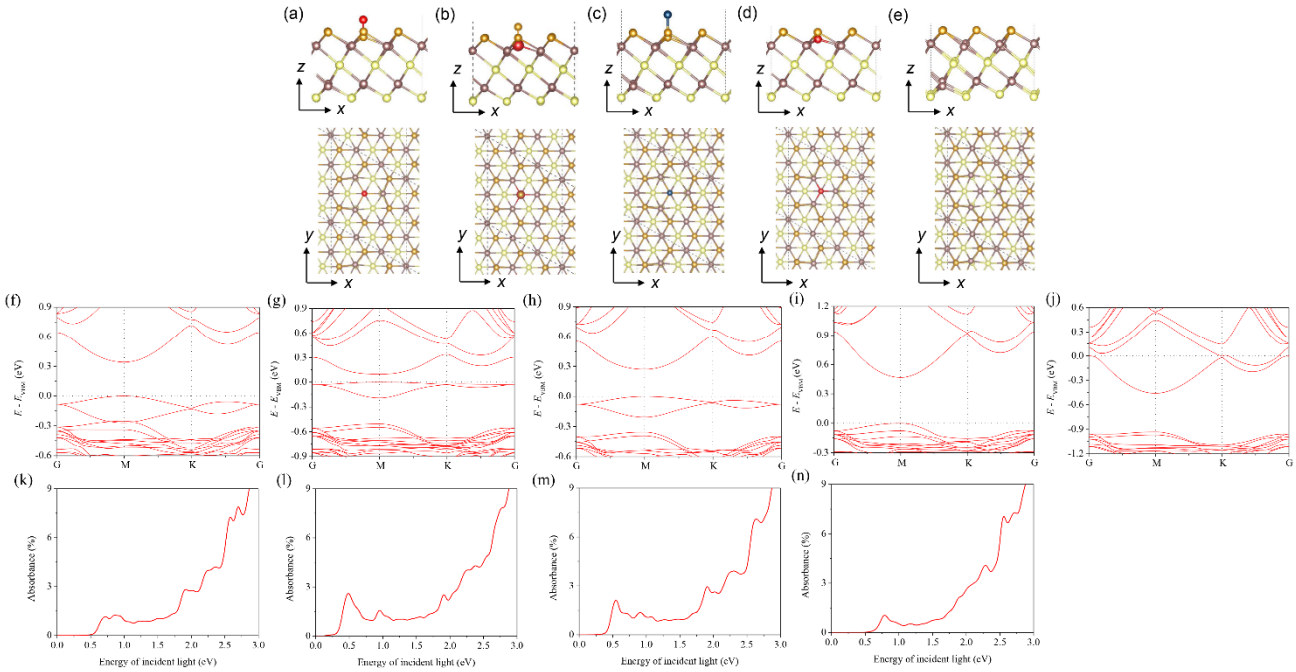

Figure S6. Geometry structures, band structures and optical absorption spectrum of monolayer defects structures. Side view and top view of (a) O-ad, (b) O–Se_as, (c) Se-ad, (d) O-Se_vac and (e) Se_vac. Band structure and optical absorption calculated by optB86b-vdW functional of (f, k) O-ad, (g, l) O–Se_as (h, m) Se-ad, (i, n) O-Se_vac and (j) Se_vac.

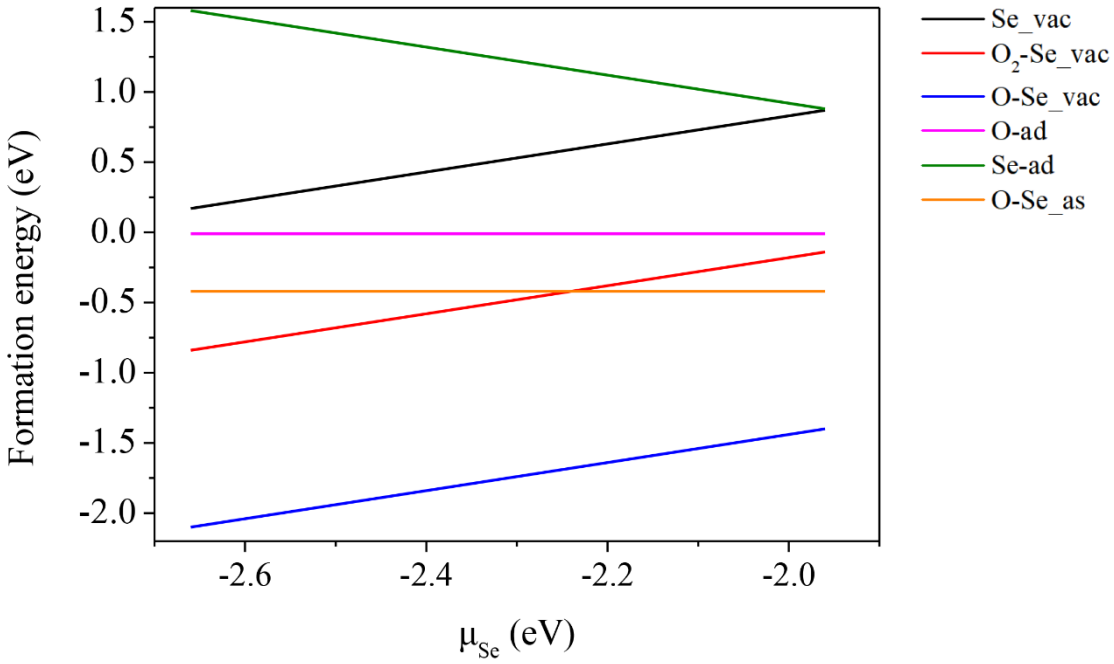

Figure S7. Formation energy of monolayer defects structures. μ_{Se} represent the energy of single Se atom.

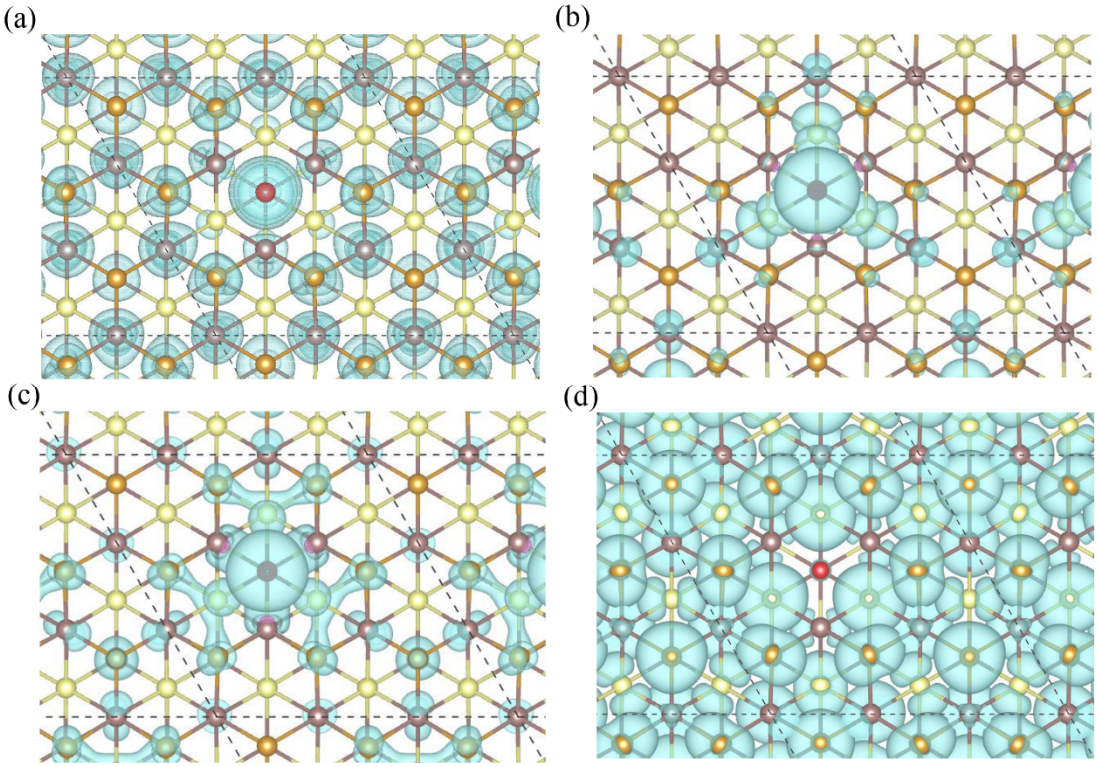

Figure S8. Visualization of wavefunctions. Top view of visualization of orbitals (a-d) CB1, VB1, VB2, VB3 of the O_2-Se_vac structure by charge density iso-surface for First Brillouin zone M point.

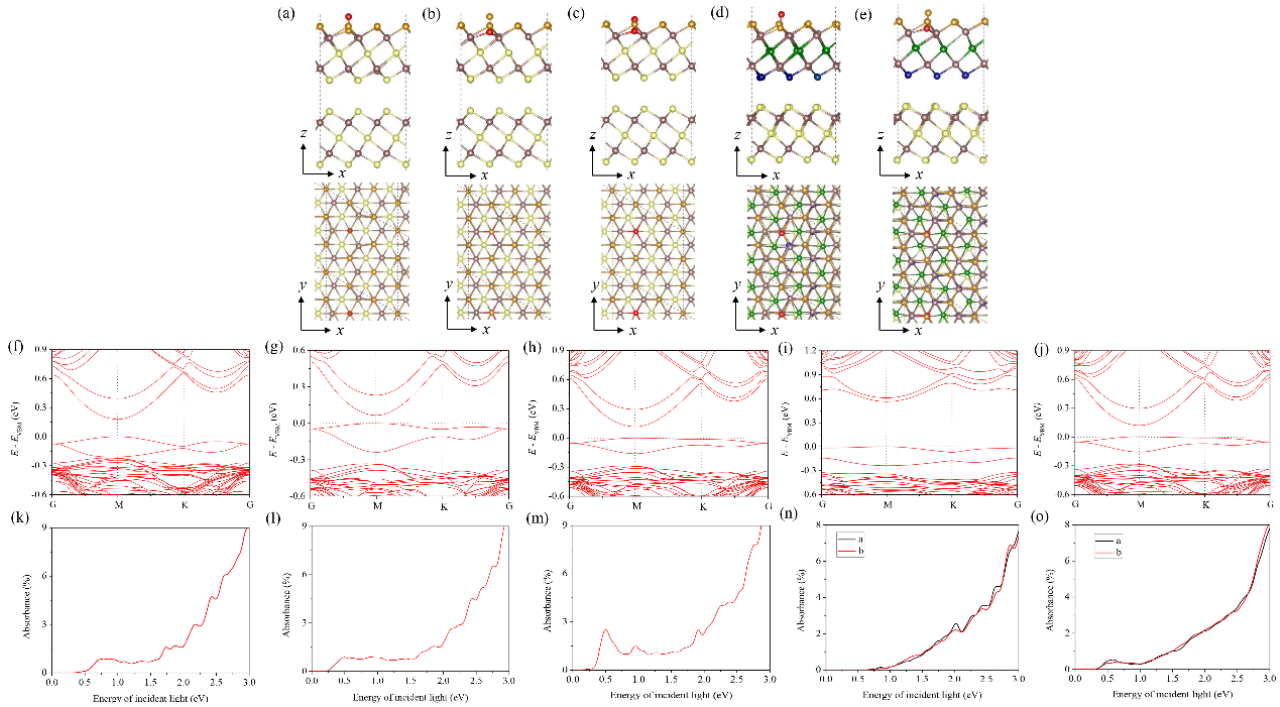

Figure S9. Geometry structures, band structures and optical absorption spectrum of five kinds of bilayer defects structures. There are two different kinds structures for O-Se_as and O-ad of bilayer defects structures: symmetry breaking (SB) and symmetry unbreaking (SUB). Side view and top view of (a) O-ad(SUB), (b) O–Se_as(SUB), (c) O_2-Se_vac, (d) O-ad(SB) and (e) O–Se_as(SB). Symmetry breaking leads to different optical absorption for different polarization light and different band gaps. Band structure and optical absorption calculated by optB86b-vdW functional of (f, k) O-ad(SUB), (g, l) O–Se_as(SUB), (h, m) O_2-Se_vac, (i, n) O-ad(SB) with bandgap 0.56 eV, absorption edge 0.64 eV and (j, o) O–Se_as (SB) with bandgap 0.12 eV, absorption edge 0.29 eV. The *a* and *b* represent light with polarization directions along different lattice base directions.

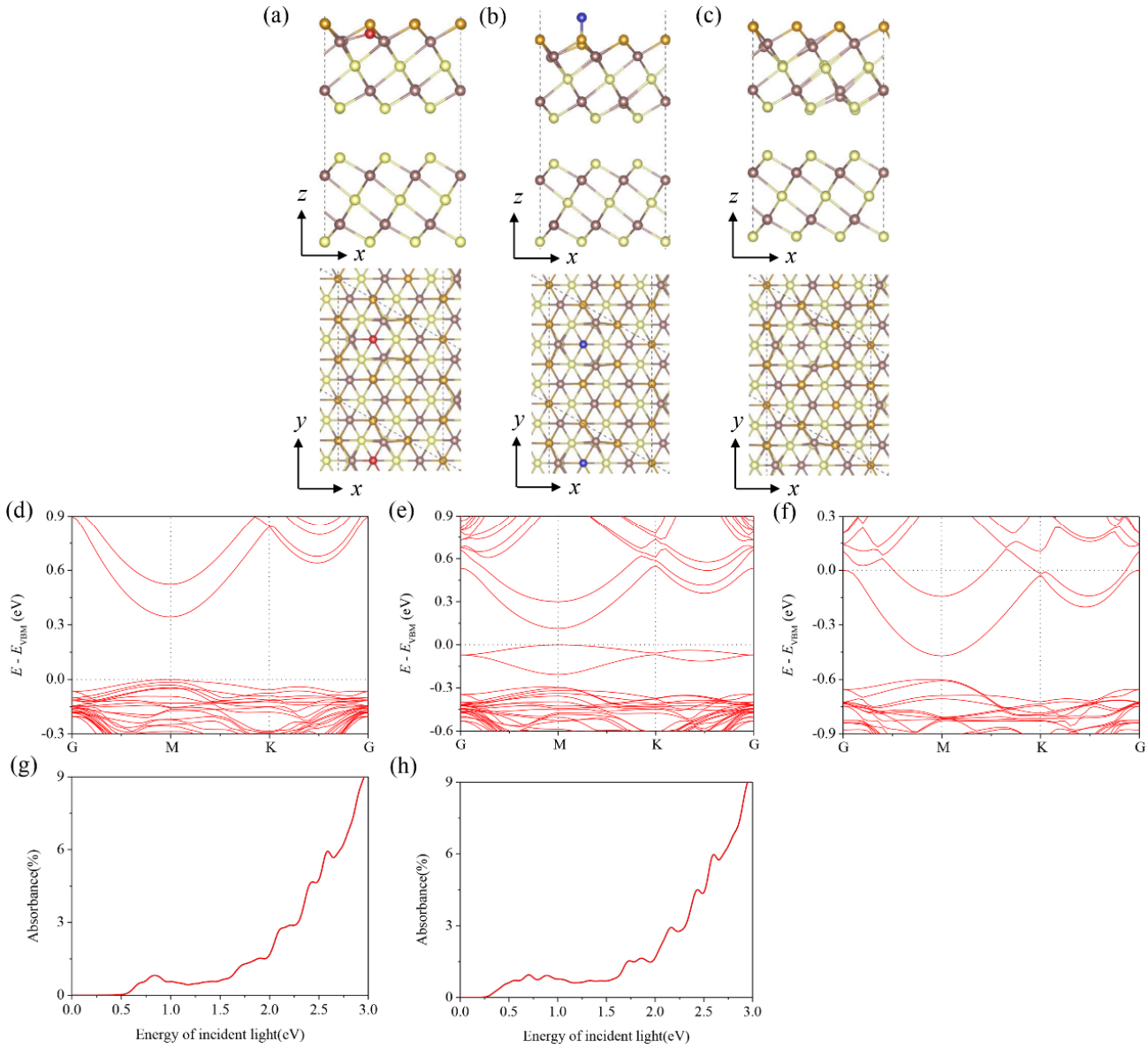

Figure S10. Geometry structures, band structures and optical absorption spectrum of other three kinds of bilayer defects structures. Side view and top view of (a) O-Se_vac, (b) Se-ad, (c) Se_vac. Band structure and optical absorption calculated by optB86b-vdW functional of (d, g) O-Se_vac, (e, h) Se-ad, (f) Se_vac.

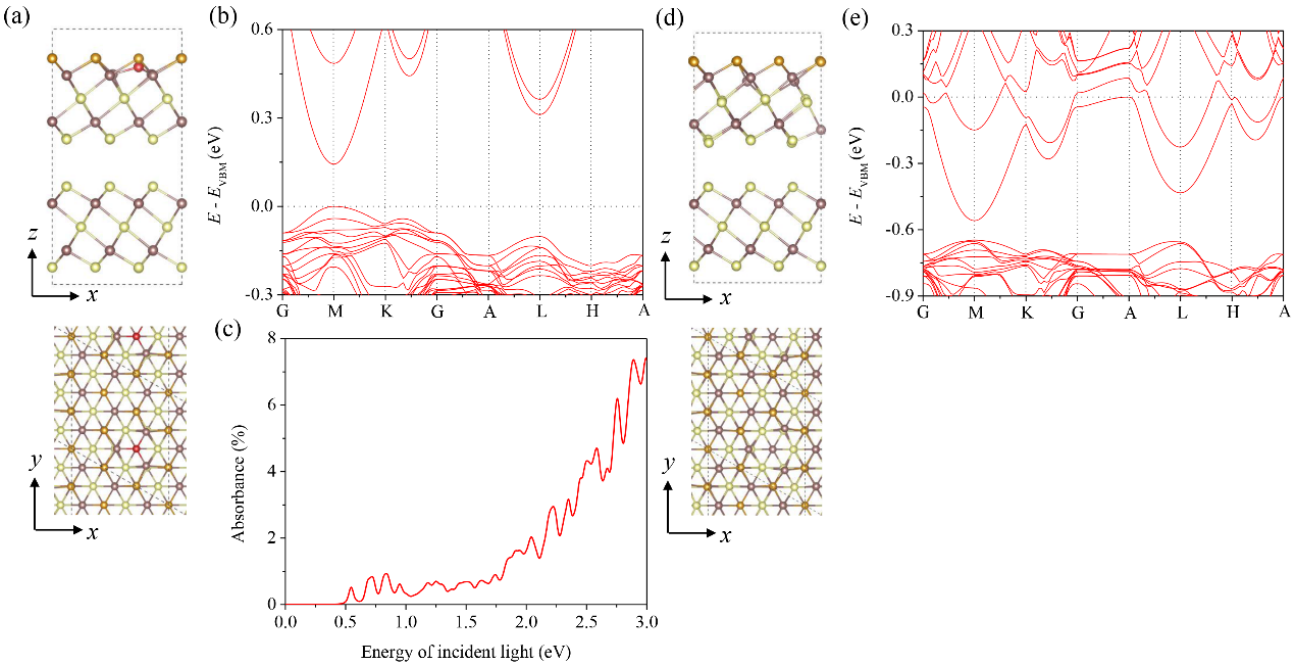

Figure S11. Geometry structures, band structures and optical absorption spectrum of bulk defects structures. Side view and top view of (a) O-Se_vac (d) Se_vac. Band structure and optical absorption calculated by optB86b-vdW functional of (b, c) O-Se_vac (e) Se_vac.

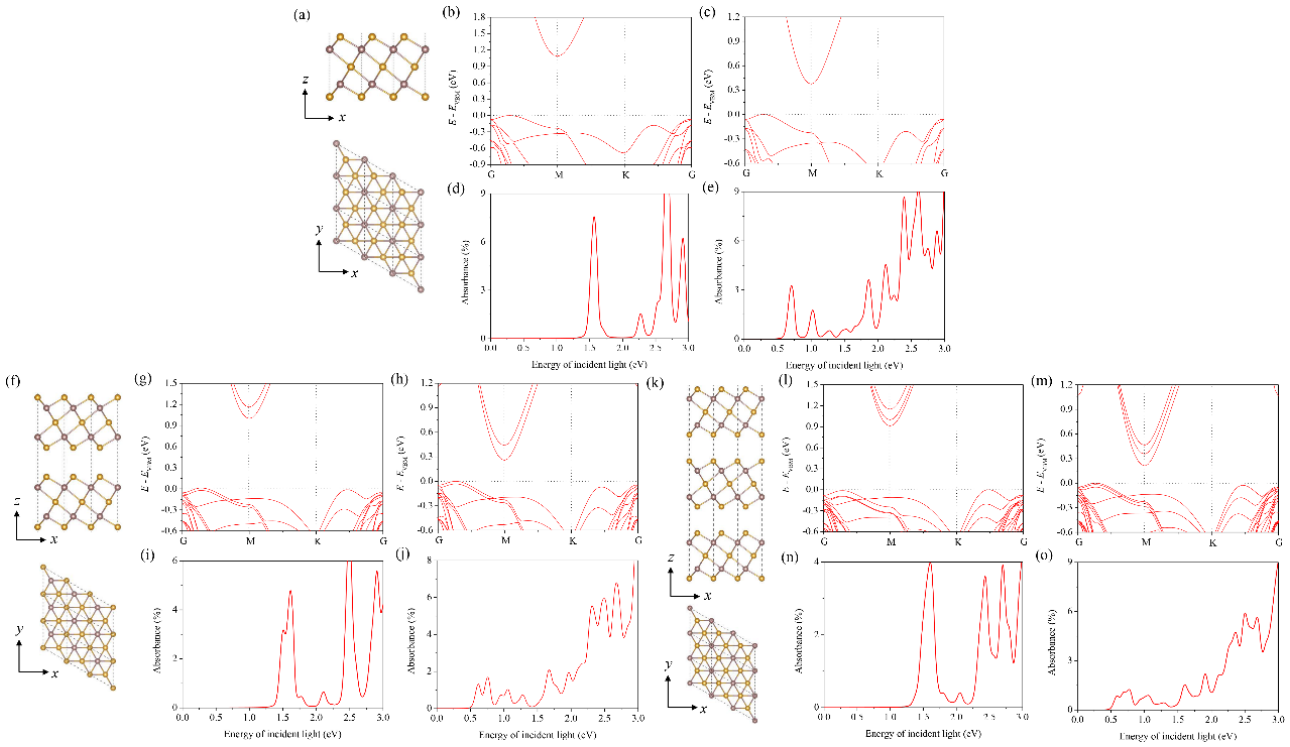

Figure S12. Geometry structures, band structures and optical absorption spectrum of monolayer, bilayer and trilayer structures. Side view and top view of (a) monolayer (f) bilayer and (k) trilayer. Band structure and optical absorption calculated by HSE06 functional of (b, d) monolayer (g, i) bilayer (l, n) trilayer with bandgap 0.91 eV and absorption edge 1.27 eV. Band structure and optical absorption calculated by optB86b-vdW functional of (c, e) monolayer (h, j) bilayer (m, o) trilayer with bandgap 0.21 eV , absorption edge 0.44 eV.

Table S1. DFT calculation results of all the structures. All calculations are taken by optB86b-vdw functional unless otherwise stated. The O-Se_as and O-ad for bilayer defects structures belong to symmetry unbreaking structure (SUB).

Gap/abs edge [eV]	Pristine(HSE06)	Pristine	Se_vac	O-Se_vac	O_2-Se_vac	Se-ad	O-ad	O-Se_as
1L	1.09 / 1.35	0.38 / 0.52	0 / 0	0.47 / 0.58	0.24 / 0.27	0.27 / 0.32	0.34 / 0.52	0.10 / 0.25
2L	0.99 / 1.30	0.26 / 0.46	0 / 0	0.34 / 0.50	0.12 / 0.20	0.11 / 0.24	0.18 / 0.37	0.07 / 0.21
Bulk	0.81 / 1.20	0.14 / 0.43	0 / 0	0.14 / 0.47	- / -	- / -	- / -	- / -
Formation energy of monolayer defects structures [eV]			0.17 ~ 0.87	-2.10 ~ -1.40	-0.84 ~ -0.14	0.88~1.58	-0.01	-0.42